
Cross-links Matter for Link Prediction: Rethinking the Debiased GNN from a Data Perspective (Supplemental Materials)

Anonymous Author(s)

Affiliation

Address

email

1 A Training Algorithm

Algorithm 1 Proposed training process

Input: Graph \mathcal{G} with link set \mathcal{E}^O . Hyper-parameters: α , β , and T , learning rate γ^O, γ^A .

Output: Node embeddings \mathbf{Z}

- 1: Randomly initialize twins GNN models with θ^O, θ^A , embedding fusion module with θ^F .
 - 2: Split \mathcal{G} into $|\mathcal{C}|$ communities and categorize links into internal-links and cross-links.
 - 3: Select augmented supervision signals \mathcal{E}^A with the highest Jaccard coefficient or co-occurrence frequency.
 - 4: **while** not converged **do**
 - 5: Compute \mathcal{L}^O and \mathcal{L}^A by Eq.(4)
 - 6: Update twins GNN models: $\theta^O \leftarrow \theta^O + \gamma^O \cdot \nabla_{\theta^O} \mathcal{L}^O$, $\theta^A \leftarrow \theta^A + \gamma^A \cdot \nabla_{\theta^A} \mathcal{L}^A$
 - 7: Compute learning rate γ_t^F and step size S_t by Eq.(8)
 - 8: **for** $step = 1$ **to** S_t **do**
 - 9: Compute \mathcal{L}^F by Eq.(7)
 - 10: Update embedding fusion module: $\theta^F \leftarrow \theta^F + \gamma_t^F \cdot \nabla_{\theta^F} \mathcal{L}^F$
 - 11: Update GNN models: $\theta^O \leftarrow \theta^O + \gamma_t^F \cdot \nabla_{\theta^O} \mathcal{L}^F$, $\theta^A \leftarrow \theta^A + \gamma_t^F \cdot \nabla_{\theta^A} \mathcal{L}^F$
 - 12: **end for**
 - 13: **end while**
 - 14: **return** \mathbf{Z}
-

2 Here we provide the pseudo codes of our training process, which are the core components helping
3 GNNs to address the bias between internal-links and cross-links without compromising utility. The
4 algorithm is also literally described in Section 3.6 for a better understanding.

5 B Further Analysis on the Role of Cross-links

6 B.1 The relationship between cross-links and information cocoons

7 To fully understand the relationship between cross-links and information cocoons, we conduct the
8 following experiments for analysis.

- 9 • **Experimental settings.** Based on the communities detected by Louvain algorithm [1] in advance,
10 we get the internal-links and cross-links of a network, and here we take Epinions and DBLP, two
11 real-world social networks as examples. The detailed dataset information is described in Section 4.1.
12 Next, we borrow the concept of message propagation from the Friedkin-Johnsen dynamics model

13 [5] and revise its formula to simulate the information propagation with randomly initialized node
 14 embeddings:

$$\mathbf{Z}_i^t = \frac{\mathbf{Z}_i^{t-1} + \sum_{j \in \mathcal{N}_i} w_{ij} \mathbf{Z}_j^{t-1}}{|\mathcal{N}_i| + 1} \quad (1)$$

15 where \mathbf{Z}_i^t denotes the embedding of node i at iteration t , and \mathcal{N}_i represent the neighbors of node i .
 16 w_{ij} is a manually controllable reweight scaler determined by the type of link $\langle i, j \rangle$. At each iteration,
 17 each node will update its embedding with the weighted average embeddings from its neighbors
 18 and itself. For simulating the lack of cross-links, we weaken the role of cross-links in information
 19 propagation by tuning the w for cross-links from 1 to 0, and setting w for internal-links to 1.

20 We further use Calinski-Harabasz(CH) index [4, 6]
 21 to measure the extent of the information cocoons
 22 phenomenon in a network, which can be calculated
 23 as follows:

$$CH_C = \frac{SSB_C(\mathbf{Z}^t)}{SSW_C(\mathbf{Z}^t)} \cdot \frac{N - C}{C - 1} \quad (2)$$

24 where SSW_C and SSB_C are functions to measure
 25 the within-cluster dispersion and between-cluster
 26 dispersion, respectively [6]. N denotes the number
 27 of nodes, and C denotes the number of communi-
 28 ties. A higher CH index score indicates that node
 29 embeddings are more polarized among communi-
 30 ties, which further illustrates the extent of the in-
 31 formation cocoon problem in the current network.

32 • **Experimental results and analysis.** In Figure C1 we show the CH index scores with node embed-
 33 dings at different propagation iteration t , and we can observe that, as the information propagation
 34 weight w for cross-links decreases, the CH index score increases consistently and far exceeds that
 35 in normal settings ($w = 1$), which indicates that the final node embeddings present more serious
 36 polarization problems among communities. Since the information in a single community is relatively
 37 limited as shown in Figure 2, the information cocoon problem actually becomes more severe with the
 38 lack of cross-links.

39 B.2 The relationship between cross-links and graph connectivity

40 With borrowing the concept of network diffusion, we try to explore the role of cross-links in graph
 41 connectivity in this part. Specifically, we apply a classic model in network diffusion: the SI model [11],
 42 to simulate the process of information propagation. In this model, each node is randomly initialized
 43 with a status called *susceptible* or *infected* at the beginning. During the diffusion iteration process, SI
 44 assumes that each infected node could infect its susceptible neighbors with probability p , and once a
 45 node becomes infected, it stays infected until the end of network diffusion, i.e. there are no more new
 46 infected nodes in a new iteration.

47 In order to provide a clear and vivid illustration, we take one of the most representative social
 48 networks – Zachary’s karate club¹ as an example. All nodes are divided into four non-overlapping
 49 communities by Louvain algorithm [1] in advance, and node #0, which stands for the instructor in
 50 this club, is initialized as the only infected node at iteration 0. We further randomly remove 80%
 51 cross-links in the graph before starting the simulation. For getting a more convincing conclusion,
 52 the network diffusion process on a graph with the same number of random edges removed is also
 53 simulated for comparison.

54 The final visualization results are shown in Figure C2. It can be seen that although we remove some
 55 edges randomly from the whole graph, the infected node #0 still propagates its information to almost
 56 all nodes in the club (red nodes in the figure) successfully. In contrast, after removing the same
 57 number of cross-links, there appears to be an obvious information isolation phenomenon, and nearly
 58 half of the nodes remain *susceptible*. In other words, cross-links play a role in bridging two different
 59 communities during network diffusion, and it would be hard for a node to send or receive messages

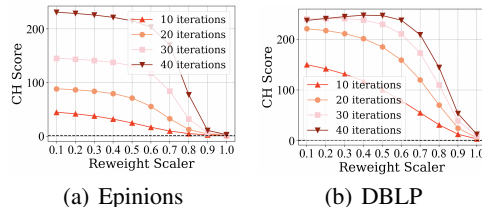


Figure C1: The distribution of CH index score
 wrt. the weight of cross-links during propaga-
 tion. A higher value indicates more severe infor-
 mation cocoons. The dashed lines indicate the
 CH index score under a normal setting.

¹https://en.wikipedia.org/wiki/Zachary%27s_karate_club

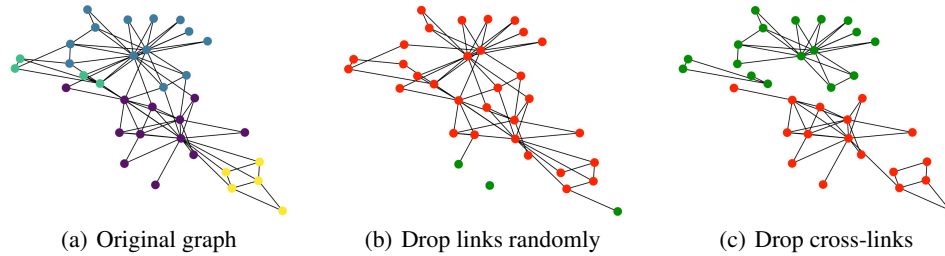


Figure C2: The visualization of diffusion simulation with SI model. Red nodes denote *infected* nodes, and green nodes represent *susceptible* nodes. (a) The original graph of the karate club. Nodes with the same color denote a community. (b) Infected graph after dropping some random edges. (c) Infected graphs after dropping some cross-links.

60 from other communities without enough cross-links. In this way, the existence of cross-links plays a
 61 key role in preserving graph connectivity.

62 C Additional Experimental Settings

63 C.1 Baselines

64 Here we introduce additional details for the base models and baselines used in our experiments.

65 (1) Base models.

- 66 • **GraphSAGE** [7]: GraphSAGE is an inductive learning framework for generating node embeddings,
 67 which samples a fixed number of neighbors during aggregation to alleviate the "neighborhood
 68 explosion" issues.
- 69 • **GIN** [20]: GIN is a graph neural network that is theoretically as powerful as the Weisfeiler-Lehman
 70 test with injective aggregation, combination, and readout functions.
- 71 • **GAT** [18]: GAT deploys the attention mechanism during aggregation to capture the neighborhood
 72 information with different weights.
- 73 • **PPRGo**[2]: By utilizing a Personalized Page Rank matrix to approximate the propagation and
 74 aggregation steps with multi-layer graph convolution, PPRGo greatly improves the efficiency and
 75 effectiveness on large graphs.
- 76 • **LightGCN** [8]: LightGCN empirically finds the redundancy of feature transformation and non-
 77 linear activation functions, and greatly simplifies the model architecture with even higher perfor-
 78 mance on the recommendation tasks.
- 79 • **UltraGCN** [14]: Based on LightGCN, UltraGCN further theoretically simplifies the model archi-
 80 tecture with approximating the infinite-layer information propagation and aggregation.

81 (2) Baselines.

- 82 • **FairWalk** [16]: Instead of random walk in node2vec, FairWalk chooses its next hop by considering
 83 the sensitive attributes in the neighborhood, which successfully mitigates the unfairness related to
 84 the sensitive attribute.
- 85 • **CFC** [3]: To ensure that the learned embeddings are not correlated with sensitive attributes, such
 86 as age or gender, CFC introduces an adversarial framework to enforce fairness constraints.
- 87 • **FairAdj** [12]: With learning to assign each edge with different weights, FairAdj generates a fair
 88 adjacency matrix and greatly improves the dyadic fairness with comparable utility in link prediction
 89 tasks.
- 90 • **FLIP** [15]: Concentrating on bursting the filter bubbles in social networks from a dyadic fairness
 91 perspective, FLIP also utilizes an adversarial learning framework to generate non-sensitive node
 92 embeddings for further link prediction.

93 • **UGE** [19]: UGE aims at learning unbiased graph embeddings from an unobserved graph, which
 94 involves no sensitive information, and further derives three kinds of variants namely UGE-w, UGE-r
 95 and UGE-c.

96 C.2 Evaluation metric.

97 In this work, we apply Hits@50, which is widely adopted in other researches [21, 22] and OGB
 98 leaderboard [9], as our main evaluation metric to measure the link prediction performance of different
 99 GNN models. The Hits@50 can be computed by:

$$Hits@50 = \frac{1}{N_{test}} \sum_{i=1}^{N_{test}} \mathbb{I}(rank_i < 50) \quad (3)$$

100 where N_{test} represents the sample size of test set, and \mathbb{I} represents an indicator function. $rank_i$
 101 denotes the similarity ranking of the i th sample.

102 C.3 Reproducibility

103 **Dataset.** For each dataset, we randomly sample and remove 5% of links in the original graph to
 104 construct the validation set and test set, and the remaining links are treated as the training set. Each
 105 true sample will be ranked among a set of 100000 randomly sampled negative links for evaluation².
 106 Note that, there is no side information, such as node features or link attributes, involved during our
 107 experiments, and we assign each node on the graph with a learnable embedding vector for training.

108 **Hyper-parameters.** As a model-agnostic framework, we deploy six kinds of GNN models as
 109 backbones, including GraphSAGE [7], GIN [20], GAT [18], PPRGo [2], LightGCN [8] and UltraGCN
 110 [14]. For all these models, we set the output embedding dimension as 64. The layer of the embedding
 111 fusion module is set to 1. The learning rates for twin GNNs are both set as 0.001 after grid search. As
 112 for the hyper-parameters in Eq.(8), α is set to be 0.005, and T is selected from {10, 25, 50} depending
 113 on the datasets and base models, and β is set to be 20. Augmentation ratio k is searched from {0.75,
 114 1.0, 1.25} for each dataset. Both weight decay and dropout rate are set to 0.

115 In particular, for GraphSAGE, we adopt a mean-pooling during aggregation; for GIN, we apply a
 116 linear layer to update node features and use max-pooling during aggregation; for GAT, we use 4
 117 attention heads in each layer; for PPRGo, we set α as 0.3, the walk length as 100; for LightGCN,
 118 we set the layer number as 2 and use the final layer’s output as embeddings; for UltraGCN, we set
 119 the number of negative samples as 64, λ as 0.8, γ as 3.5. Our implementation code and datasets are
 120 released anonymously in https://anonymous.4open.science/r/Neurips2023_9342/.

121 For Fairwalk, we follow the settings in the original paper and set the walk number to 20, and the
 122 window length to 80; for CFC, we set the training steps of the discriminator as 5; for FairAdj, we
 123 set T_2 to 15 and λ to 10; for FLIP, we take the suggestions in the original implementation, and the
 124 settings are $\alpha(0.1)$, $\beta(0.2)$; for UGE, we deploy the weighting-based variant as our baseline given
 125 that there is no non-sensitive attribute in our settings.

126 C.4 Details on LastFM dataset

127 Due to the heterogeneity of the recommendation
 128 datasets, it’s hard to directly deploy community
 129 detection algorithms on the original networks
 130 and define the corresponding internal-links and
 131 cross-links. To this end, inspired by ItemCF
 132 [13, 17], we first generate an item-item graph
 133 according to the co-occurrence relationship. For
 134 example, given a pair of items $\langle v_1, v_2 \rangle$, if
 135 they both have interactions with user u at least
 136 O times, where O is a hyperparameter to control
 137 the confidence of generated item-item graph,
 138 there will form a link between v_1 and v_2 . Next,

Table C1: The comparison between our implemen-
 tations and normal implementations on LastFM.
 The average results are reported after repeating
 each method five times.

		LastFM (Hits@50)
LightGCN	Original	29.82% \pm 0.25
	Ours	29.30% \pm 0.21
UltraGCN	Original	28.50% \pm 0.28
	Ours	27.32% \pm 0.19

²Here we follow the evaluation protocol in OGB [9], which is widely used in research.

139 we can deploy our framework on the generated item-item graph for learning debiased item em-
 140 beddings $\mathbf{I} \in \mathbb{R}^{|V| \times D}$, where $|V|$ represents the number of items and D represents the embedding
 141 dimension. After that, item similarity matrix $\mathbf{I}^2 \in \mathbb{R}^{|V| \times |V|}$ is calculated, which is further used for
 142 the final recommendation:

$$\mathbf{P} = \mathbf{A} \times \mathbf{I}^2 \quad (4)$$

143 where $\mathbf{P} \in \mathbb{R}^{|U| \times |V|}$ denotes the predicted confidence matrix between users and items, and $\mathbf{A} \in$
 144 $\mathbb{R}^{|U| \times |V|}$ represents the adjacency matrix of the original user-item graph.

145 In order to prove that our implementation will not affect the performance of the original GNN
 146 models, we compared our implementation (denoted as "Ours"), where O is set to be 1, with GNNs
 147 trained on the user-item graph normally (denoted as "Original") in Table C1. The results indicate
 148 that our implementation does not sacrifice the capability of base GNN models severely to adapt our
 149 framework.

150 D Further Experiments and Analysis

151 D.1 Hyper-parameter Analysis

152 As the core component in our frame-
 153 work, supervision augmentation plays a
 154 key role in mitigating the bias between
 155 internal-links and cross-links. To explore
 156 its impact in a finer granularity, we vary
 157 the augmentation ratio k and see how
 158 the performance of our method changes.
 159 Specifically, we take LightGCN as the
 160 base model and investigate the perfor-
 161 mance on internal-links (Internal.), cross-
 162 links (Cross.) and the whole link set
 163 (Overall) by varying k in $\{0, 0.25, 0.5,$
 164 $0.75, 1, 1.25\}$. Without losing generality,
 165 here we take Jaccard based supervision augmentation. As shown in Figure C3, the performance of
 166 the two kinds of links increasingly improves as k grows, accompanied by a steady decrease in the
 167 difference between them. This is expected because we introduce a large amount of augmented cross-
 168 links signals to mitigate the bias. And when k reaches 1, which means $|\mathcal{E}_{in}| \approx |\mathcal{E}_{cr}|$, the framework
 169 gradually converges to a stable status. Empirically, a setting $k = 1$ would be a near-optimal option.

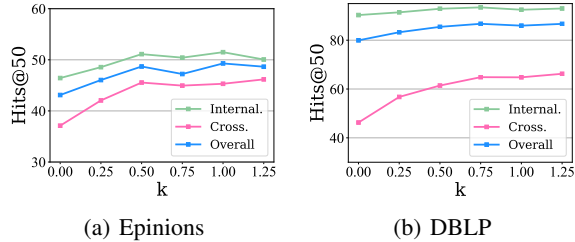


Figure C3: The impact of augmentation size

170 D.2 Alternative Community Detection Algorithm

171 In this part, we aim to conduct an
 172 ablation study on different commu-
 173 nity detection methods to prove the
 174 usefulness of our proposed frame-
 175 work. Since we emphasize the bias
 176 from a topological perspective, we
 177 prefer to use the community detec-
 178 tion algorithm based on graph struc-
 179 ture. Specifically, to illustrate the
 180 universality of our framework, we
 181 conduct experiments based on the
 182 METIS [10] algorithm as an ablation
 183 study, and the results on three GNNs
 184 are shown in Table C2. Specifically, the number of communities is set to be 50 in advance for METIS,
 185 and all other hyper-parameters are set to be the same as that in Louvain-based experiments, which
 186 can be found in Section B.3. All results are based on Jaccard based augmentation.

Table C2: Ablation study with METIS community detection algorithm on two real-world datasets. The results (Hits@50) are reported in percentage (%). We **bold** the results when our framework improves the base GNN model.

		Epinions				DBLP			
		Internal.↑	Cross.↑	Overall↑	Bias↓	Internal.↑	Cross.↑	Overall↑	Bias↓
SAGE	Orig.	36.97	19.48	30.75	17.49	69.80	19.00	54.28	50.80
	Debias	39.06	28.93	35.89	10.13	78.67	34.65	65.22	44.02
GAT	Orig.	38.33	34.77	37.15	3.56	68.62	28.15	56.26	40.47
	Debias	39.96	36.88	38.86	3.08	75.94	42.77	65.81	33.17
UltraGCN	Orig.	27.27	11.62	20.77	15.65	97.34	70.57	89.16	26.77
	Debias	46.92	38.18	44.04	8.74	97.47	73.67	90.20	23.80

187 The results indicate that, although we change the community detection algorithm, our framework
 188 still successfully mitigates the bias between internal-links and cross-links, and achieves competitive
 189 results compared with the Louvain-based results, which verifies our work's compatibility.

190 **D.3 Supervision Augmentation Analysis**

191 In Section 3.3, we design two kinds of data augmentation methods for generating pseudo cross-links
 192 supervision signals. Intuitively, if the pseudo supervision signals have a high confidence level, they
 193 can provide significant benefits to our framework. To this end, we aim to verify our hypothesis and
 194 analyze the impact of different supervision augmentation methods on our framework.

195 We first statistic the average hop distance between the node pairs generated with different supervision aug-
 196 mentation methods. As shown in Table C3, since we only choose node pairs with the most common neigh-
 197 bors in Jaccard based augmentation, the hop distance is fixed to 2. When we use random walk based augmen-
 198 tation, the average distance increases consistently on two datasets, which verifies its effectiveness in covering
 199 nodes that are not located in the boundary of communities.

200 Table C4 further presents the performance of our framework with random walk based augmentation,
 201 which is literally described in Section 3.3. Specifically, for providing fair comparison, all hyper-parameters
 202 in random walk based experiments, including augmentation ratio k and others are set to be the same as that
 203 in Jaccard based experiments. Compared to Table 2, it can be shown that the random walk based framework
 204 shows less improvement on cross-links, which results in worse debias results. This observation can be
 205 explained by the hop distance in Table C3, which implies that the random walk based augmentation
 206 may have lower confidence due to the longer topological distance between node pairs. However,
 207 compared with the base GNNs, the random walk based framework can still consistently reduce the
 208 bias between internal-links and cross-links with improved overall performance.

Table C3: The average hop distance between node pairs generated by different supervision augmentation methods.

	Epinions	DBLP
Jaccard based	2.00	2.00
Random walk based	2.69	3.14

Table C4: Link prediction performance (Hits@50) of internal-links, cross-links and the whole link set of our methods with random walk based augmentation and corresponding base models on two real-world datasets. The results are reported in percentage (%). We **bold** the results when our framework improves the base GNN model.

		Epinions				DBLP			
		Internal.↑	Cross.↑	Overall↑	Bias↓	Internal.↑	Cross.↑	Overall↑	Bias↓
SAGE	Orig.	31.68	28.91	30.69	2.77	69.27	14.62	56.41	54.65
	Fair.	31.72	29.17	31.28	2.55	80.28	28.63	68.12	51.65
GIN	Orig.	33.49	30.97	32.59	2.52	56.66	16.86	47.29	39.80
	Fair.	38.35	36.89	37.12	1.46	68.12	32.07	59.64	36.05
GAT	Orig.	39.30	34.90	37.73	4.40	66.25	22.47	55.94	43.78
	Fair.	40.02	36.29	37.98	3.73	75.03	32.18	64.94	42.85
PPRGo	Orig.	42.86	28.75	37.83	14.11	85.71	41.14	75.28	44.58
	Fair.	45.36	40.12	43.49	5.24	90.48	49.51	80.47	42.08
LightGCN	Orig.	46.43	37.11	43.11	9.32	85.95	47.41	76.88	38.54
	Fair.	48.15	40.45	45.41	7.65	92.16	57.55	84.01	34.61
UltraGCN	Orig.	30.62	5.81	21.78	24.81	95.74	63.82	88.22	31.92
	Fair.	52.16	51.99	52.10	0.17	96.47	66.25	89.35	30.22

226 **References**

227 [1] V. D. Blondel, J.-L. Guillaume, R. Lambiotte, and E. Lefebvre. Fast unfolding of communities
 228 in large networks. *Journal of statistical mechanics: theory and experiment*, 2008(10):P10008,
 229 2008.

230 [2] A. Bojchevski, J. Klicpera, B. Perozzi, A. Kapoor, M. Blais, B. Rózemberczki, M. Lukasik,
 231 and S. Günnemann. Scaling graph neural networks with approximate pagerank. In R. Gupta,
 232 Y. Liu, J. Tang, and B. A. Prakash, editors, *KDD '20: The 26th ACM SIGKDD Conference on*
 233 *Knowledge Discovery and Data Mining, Virtual Event, CA, USA, August 23-27, 2020*, pages
 234 2464–2473. ACM, 2020.

235 [3] A. J. Bose and W. L. Hamilton. Compositional fairness constraints for graph embeddings. In
 236 K. Chaudhuri and R. Salakhutdinov, editors, *Proceedings of the 36th International Conference*
 237 *on Machine Learning, ICML 2019, 9-15 June 2019, Long Beach, California, USA*, volume 97
 238 of *Proceedings of Machine Learning Research*, pages 715–724. PMLR, 2019.

239 [4] T. Caliński and J. Harabasz. A dendrite method for cluster analysis. *Communications in*
 240 *Statistics-theory and Methods*, 3(1):1–27, 1974.

241 [5] U. Chitra and C. Musco. Analyzing the impact of filter bubbles on social network polarization.
 242 In J. Caverlee, X. B. Hu, M. Lalmas, and W. Wang, editors, *WSDM '20: The Thirteenth ACM*

- 243 *International Conference on Web Search and Data Mining, Houston, TX, USA, February 3-7,*
244 *2020, pages 115–123. ACM, 2020.*
- 245 [6] Y. Ge, S. Zhao, H. Zhou, C. Pei, F. Sun, W. Ou, and Y. Zhang. Understanding echo chambers
246 in e-commerce recommender systems. In *Proceedings of the 43rd International ACM SIGIR*
247 *conference on research and development in Information Retrieval, SIGIR 2020, Virtual Event,*
248 *China, July 25-30, 2020, pages 2261–2270. ACM, 2020.*
- 249 [7] W. L. Hamilton, Z. Ying, and J. Leskovec. Inductive representation learning on large graphs.
250 In *Advances in Neural Information Processing Systems 30: Annual Conference on Neural*
251 *Information Processing Systems 2017, December 4-9, 2017, Long Beach, CA, USA, pages*
252 *1024–1034, 2017.*
- 253 [8] X. He, K. Deng, X. Wang, Y. Li, Y. Zhang, and M. Wang. Lightgcn: Simplifying and powering
254 graph convolution network for recommendation. In *Proceedings of the 43rd International ACM*
255 *SIGIR conference on research and development in Information Retrieval, SIGIR 2020, Virtual*
256 *Event, China, July 25-30, 2020, pages 639–648. ACM, 2020.*
- 257 [9] W. Hu, M. Fey, M. Zitnik, Y. Dong, H. Ren, B. Liu, M. Catasta, and J. Leskovec. Open graph
258 benchmark: Datasets for machine learning on graphs. In H. Larochelle, M. Ranzato, R. Hadsell,
259 M. Balcan, and H. Lin, editors, *Advances in Neural Information Processing Systems 33: Annual*
260 *Conference on Neural Information Processing Systems 2020, NeurIPS 2020, December 6-12,*
261 *2020, virtual, 2020.*
- 262 [10] G. Karypis and V. Kumar. A fast and high quality multilevel scheme for partitioning irregular
263 graphs. *SIAM J. Sci. Comput.*, 20(1):359–392, 1998.
- 264 [11] W. O. Kermack and A. G. McKendrick. A contribution to the mathematical theory of epidemics.
265 *Proceedings of the royal society of london. Series A, Containing papers of a mathematical and*
266 *physical character*, 115(772):700–721, 1927.
- 267 [12] P. Li, Y. Wang, H. Zhao, P. Hong, and H. Liu. On dyadic fairness: Exploring and mitigating
268 bias in graph connections. In *9th International Conference on Learning Representations, ICLR*
269 *2021, Virtual Event, Austria, May 3-7, 2021. OpenReview.net, 2021.*
- 270 [13] G. Linden, B. Smith, and J. York. Amazon.com recommendations: Item-to-item collaborative
271 filtering. *IEEE Internet Comput.*, 7(1):76–80, 2003.
- 272 [14] K. Mao, J. Zhu, X. Xiao, B. Lu, Z. Wang, and X. He. Ultragcn: Ultra simplification of graph
273 convolutional networks for recommendation. In *CIKM '21: The 30th ACM International*
274 *Conference on Information and Knowledge Management, Virtual Event, Queensland, Australia,*
275 *November 1 - 5, 2021, pages 1253–1262. ACM, 2021.*
- 276 [15] F. Masrour, T. Wilson, H. Yan, P. Tan, and A. Esfahanian. Bursting the filter bubble: Fairness-
277 aware network link prediction. In *The Thirty-Fourth AAAI Conference on Artificial Intelligence,*
278 *AAAI 2020, The Thirty-Second Innovative Applications of Artificial Intelligence Conference,*
279 *IAAI 2020, The Tenth AAAI Symposium on Educational Advances in Artificial Intelligence,*
280 *EAAI 2020, New York, NY, USA, February 7-12, 2020, pages 841–848. AAAI Press, 2020.*
- 281 [16] T. Rahman, B. Surma, M. Backes, and Y. Zhang. Fairwalk: Towards fair graph embedding.
282 In *Proceedings of the Twenty-Eighth International Joint Conference on Artificial Intelligence,*
283 *IJCAI-19, pages 3289–3295. International Joint Conferences on Artificial Intelligence Organi-*
284 *zation, 7 2019.*
- 285 [17] Y. Shen, Y. Wu, Y. Zhang, C. Shan, J. Zhang, K. B. Letaief, and D. Li. How powerful is graph
286 convolution for recommendation? In G. Demartini, G. Zuccon, J. S. Culpepper, Z. Huang,
287 and H. Tong, editors, *CIKM '21: The 30th ACM International Conference on Information and*
288 *Knowledge Management, Virtual Event, Queensland, Australia, November 1 - 5, 2021, pages*
289 *1619–1629. ACM, 2021.*
- 290 [18] P. Velickovic, G. Cucurull, A. Casanova, A. Romero, P. Liò, and Y. Bengio. Graph attention
291 networks. In *6th International Conference on Learning Representations, ICLR 2018, Vancouver,*
292 *BC, Canada, April 30 - May 3, 2018, Conference Track Proceedings. OpenReview.net, 2018.*

- 293 [19] N. Wang, L. Lin, J. Li, and H. Wang. Unbiased graph embedding with biased graph observations.
294 In F. Laforest, R. Troncy, E. Simperl, D. Agarwal, A. Gionis, I. Herman, and L. Médini, editors,
295 *WWW '22: The ACM Web Conference 2022, Virtual Event, Lyon, France, April 25 - 29, 2022*,
296 pages 1423–1433. ACM, 2022.
- 297 [20] K. Xu, W. Hu, J. Leskovec, and S. Jegelka. How powerful are graph neural networks? In *7th*
298 *International Conference on Learning Representations, ICLR 2019, New Orleans, LA, USA,*
299 *May 6-9, 2019*. OpenReview.net, 2019.
- 300 [21] S. Yun, S. Kim, J. Lee, J. Kang, and H. J. Kim. Neo-gnns: Neighborhood overlap-aware graph
301 neural networks for link prediction. In M. Ranzato, A. Beygelzimer, Y. N. Dauphin, P. Liang,
302 and J. W. Vaughan, editors, *Advances in Neural Information Processing Systems 34: Annual*
303 *Conference on Neural Information Processing Systems 2021, NeurIPS 2021, December 6-14,*
304 *2021, virtual*, pages 13683–13694, 2021.
- 305 [22] M. Zhang, P. Li, Y. Xia, K. Wang, and L. Jin. Labeling trick: A theory of using graph neural
306 networks for multi-node representation learning. In M. Ranzato, A. Beygelzimer, Y. N. Dauphin,
307 P. Liang, and J. W. Vaughan, editors, *Advances in Neural Information Processing Systems 34:*
308 *Annual Conference on Neural Information Processing Systems 2021, NeurIPS 2021, December*
309 *6-14, 2021, virtual*, pages 9061–9073, 2021.